

MHD simulations of the interaction of the solar wind with a fast-rotating planet (e.g. Saturn or Uranus)

L. Griton and F. Pantellini

LESIA, Observatoire de Paris, PSL Research University, CNRS, Sorbonne Universités, UPMC Univ. Paris 06, Univ. Paris Diderot, Sorbonne Paris Cité

Abstract

We present 3D magnetohydrodynamics (MHD) simulations (on a spherical grid) of the interaction of the solar wind with a fast rotating magnetized planet, with arbitrary orientation of magnetic and spin axis. The large-scale flow in fast-rotating magnetospheres (e.g. the giant planets of the solar system) is described here for different orientations of the interplanetary magnetic field. We present in particular the effects of rotation on the configuration of the planet-connected magnetic field lines and on the flow pattern. We adapted the MPI-AMRVAC code to allow for any possible orientation of spin and magnetic axis using a background/residual decomposition of the magnetic field. The Saturn-like case is briefly discussed.

1. Introduction

Our aim is to simulate the interaction between a supersonic magnetised solar wind and a fast rotating planet with strong intrinsic magnetic field and arbitrary orientations of the magnetic and spin axis.

2. Methods

We run the AMRVAC code in spherical geometry. The simulation domain is bounded by two concentric spherical shells (see Fig.1). The inner shell (generally assumed to be the planet surface) is rotating around an axis going through its center. The outer boundary is an inertial one with the solar wind flowing in, along the negative z direction.

2.1. MHD definition of a fast rotator

Let R_M be the subsolar distance of the magnetopause (see Fig.2) which we assume to be the point where the solar wind dynamic pressure and the planetary (dipolar) magnetic field do equilibrate. R_M being a characteristic dimension of the magnetosphere, we can define a characteristic crossing time for Alfvén waves

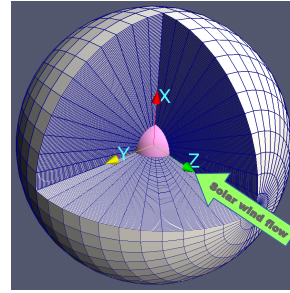


Figure 1: Simulation domain (spherical grid) contained within two spherical shells. The Z axis is defined as the solar wind flow anti-direction.

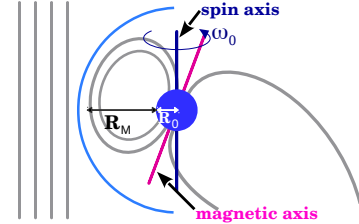


Figure 2: Schematic of a planetary magnetosphere, with R_M the distance between the planet surface and the subsolar position of the magnetopause, and ω_0 the angular spin velocity.

$t_A = R_M/v_A$ (with v_A the Alfvén waves velocity) and compare this time with the characteristic rotation time $t_\omega \simeq 1/\omega_0$. By arbitrary assuming t_ω as the time for a 5 degree rotation, we use the dimensionless parameter $\eta = t_A/t_\omega$ to characterize fast and slow rotators. Assuming a dipolar planetary potential field (decreasing as R^{-3}), we obtain:

$$\eta = \frac{t_A}{t_\omega} = \frac{36}{\pi} \Omega \left(\frac{R_M}{R_0} \right)^4 \quad (1)$$

where $\Omega = \omega_0 R_0/v_{A0}$ (ω_0 : angular velocity, R_0 : radius of the planet, v_{A0} : Alfvén velocity at the sur-

face and magnetic equator). If $\eta \geq 1$, the planetary rotation is fast and plays its part in the structure of the magnetosphere. If $\eta \ll 1$, rotation is too slow to affect in a significant way the magnetosphere.

2.2. $\mathbf{B}_0 + \mathbf{B}_1$ decomposition of the planetary field

We use AMRVAC to solve the full system of MHD equations (see [1],[2]) with the newly added possibility to split the magnetic field \mathbf{B} into the sum of analytic background field \mathbf{B}_0 (in our case an approximation of the planetary field) and perturbation field \mathbf{B}_1 (as in [3] where \mathbf{B}_0 was assumed to be potential). MHD causality, however, requires fluid motions not to exceed the fast speed with respect to the frame where \mathbf{B}_0 is at rest. Thus \mathbf{B}_0 is compressed between the inner boundary and a radial distance R (see Fig.3).

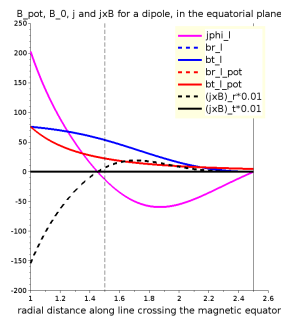


Figure 3: Planetary magnetic field intensity (blue curve) used as background field \mathbf{B}_0 as a function of the radial distance along a line crossing the magnetic equator. The profile has been obtained by suitably compressing a potential dipolar field (red curve) inside a spherical shell located at $R = 2.5$. The associated current density j is shown in magenta and the $\mathbf{j} \times \mathbf{B}$ force as a black dashed curve. Distances are normalized to R_0 , field intensities are in arbitrary units.

3. Application to a fast-rotating planet (Saturn's configuration)

The left panel of Fig. 4 shows the steady-state flow pattern (arrows) in the equatorial plane for the case of a Saturn-like configuration where spin axis and magnetic axis are aligned. The solar wind flows in from the right with its magnetic field oriented antiparallel with respect to the equatorial planetary field.

The grey scale is for density which allows to identify, from right to left, a darkening at the shock ramp, where density increases, followed by a density drop at the magnetopause (also characterized by counterstreaming flows on the dawn side). The simulation has been realized using the $\mathbf{B}_0 + \mathbf{B}_1$ decomposition shortly described in subsection 2.2. The right panel of Fig. 4 illustrates the $\mathbf{B}_0 + \mathbf{B}_1$ decomposition along the subsolar direction.

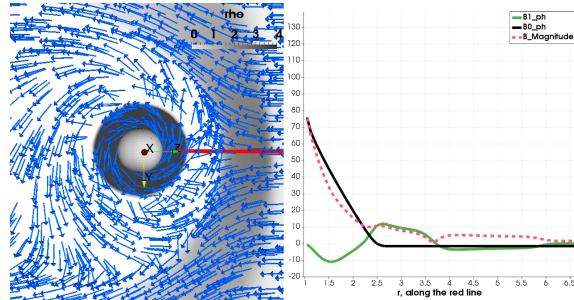


Figure 4: Left panel: plasma flow in the equatorial plane of a Saturn-like planetary magnetosphere. Arrows represent the plasma flow and the grey scale is for the plasma density. Right panel: out of the plane components of the B_0 (black) and B_1 (green) components of the magnetic field (pink dashed line) along the subsolar direction (red line in left panel).

4. Summary and Conclusions

Fast rotating planets with strong intrinsic magnetic fields can be conveniently simulated in an inertial frame by introducing a time-dependent non-potential \mathbf{B}_0 field into the MHD equations. We have illustrated the procedure for the case of a steady state Saturn-like planet.

References

- [1] R. Keppens, Z. Meliani, A.J. van Marle, P. Delmont, A. Vlasis and B. van der Holst. *Journal of Computational Physics*, 231-3-p. 718 - 744, 2012.
- [2] F. Pantellini, L. Griton, and J. Varela. *Planetary and Space Science*, 112:1–9, July 2015.
- [3] T. Tanaka *Journal of computational physics* **111**, 389-389 (1994)